CHEMISTRY OF MATERIALS
Article

Chem. Mater. **2010,** *22,* 1263–1270 1263
DOI:10.1021/cm902713m

Li_2O Removal from Li_5FeO_4: A Cathode Precursor for Lithium-Ion Batteries†

C. S. Johnson,*,‡ S.-H. Kang,‡ J. T. Vaughey,‡ S. V. Pol,⊥ M. Balasubramanian,⊥ and M. M. Thackeray‡

‡*Electrochemical Energy Storage Department, Chemical Sciences and Engineering Division and* ⊥*Advanced Photon Source, Argonne National Laboratory, Argonne, Illinois 60439*

Received September 1, 2009. Revised Manuscript Received December 2, 2009

Lithium has been extracted both electrochemically and chemically from the defect antifluorite-type structure, Li_5FeO_4 ($5Li_2O \cdot Fe_2O_3$). The electrochemical data show that four lithium ions can be removed from Li_5FeO_4 between 3.5 and 4.5 V. vs Li^0. X-ray absorption spectroscopy (XAS) data of electrochemically delithiated samples show evidence of some Fe^{3+} to Fe^{4+} oxidation during the initial charge. On the other hand, XAS data of chemically delithiated samples show no evidence of Fe^{3+} to Fe^{4+} oxidation, but rather a change in coordination of the Fe^{3+} ions from tetrahedral to octahedral coordination, suggesting that lithium extraction from Li_5FeO_4 is accompanied predominantly by the release of oxygen, the net loss being lithia (Li_2O); the residual lithium-iron-oxide product has a Fe_2O_3-rich composition. The high lithium content in Li_5FeO_4 renders it an attractive cathode precursor for loading the graphite (C_6) anode of lithium-ion electrochemical cells with sufficient lithium to enable the discharge of a charged component in the parent cathode, $Li_{1.2}V_3O_8$, as well as the residual Fe_2O_3-rich component. The electrochemical behavior of $C_6/Li_5FeO_4-Li_{1.2}V_3O_8$ lithium-ion cells is compared to $C_6/Li_2MnO_3-Li_{1.2}V_3O_8$ cells containing a layered Li_2MnO_3 ($Li_2O \cdot MnO_2$) cathode precursor with a lower Li_2O content, from which lithia can be extracted at higher potentials, typically > 4 V vs metallic lithium. The ability to remove Li_2O electrochemically from metal oxide host structures with a high lithium content, such as Li_5FeO_4, has implications for Li-air cells.

I. Introduction

The application of charged cathodes, such as MnO_2, V_2O_5, or $Li_{1.2}V_3O_8$ that offer high theoretical capacities (300−440 mAh/g) in conventional lithium-ion cells with graphite anodes is prohibited because there is no, or insufficient, lithium in the cathode to lithiate the anode during the first charge. It has recently been demonstrated that Li_2MnO_3 ($Li_2O \cdot MnO_2$)[1,2] with a layered rock salt structure and structurally integrated materials containing an Li_2MnO_3 component, such as $xLi_2MnO_3 \cdot (1-x)LiMO_2$ (M = Mn, Ni, Co)[3] and $xLi_2MnO_3 \cdot (1-x)LiM'_2O_4$ (M' = Mn, Ni, Li),[4] can be electrochemically charged by removing Li_2O to yield an active MnO_2 component. Because oxygen is irreversibly lost from the Li_2MnO_3 structure during this process, only one of the two lithium ions can be reintroduced into the residual MnO_2 structure during the reverse reaction to yield the corresponding rocksalt stoichiometry, $LiMnO_2$. The surplus lithium loaded into the anode can therefore be used either to compensate for irreversible capacity loss effects at carbon, metal (e.g., Sn), intermetallic (e.g., Cu_6Sn_5) or metalloid (e.g., Si) anodes or, alternatively, to lithiate a charged component in the parent cathode material. The latter principle has already been demonstrated, for example, in structurally integrated $xLi_2MnO_3 \cdot (1-x)Li_{1+x}Mn_{2-x}O_4$[5] and $\{Li_2MnO_3 \cdot LiMn_{0.5}Ni_{0.5}O_2\} \cdot LiMn_{1.5}Ni_{0.5}O_4$[6] electrodes and blended $\{0.6Li_2MnO_3 \cdot 0.4LiMn_{0.333}Ni_{0.333}Co_{0.333}O_2\} \cdot V_2O_5$ electrodes,[7] in which $Li_{1+x}Mn_{2-x}O_4$, $LiMn_{1.5}Ni_{0.5}O_4$, and V_2O_5 represent the charged components of the electrodes, respectively.

In this paper, we explore the possibility of using an antifluorite Li_5FeO_4 ($5Li_2O \cdot Fe_2O_3$) cathode precursor as a source of lithium for loading the graphite anode of lithium-ion cells during the cell charging. This approach is an attractive alternative to (1) using commercial lithium metal powder or foil as a means to prelithiate graphite anodes when lithium-ion cells are loaded in the charged state,[8] or (2) having to lithiate charged cathodes prior to

† Accepted as part of the 2010 "Materials Chemistry of Energy Conversion Special Issue".

*Author to whom correspondence should be addressed. E-mail: cjohnson@anl.gov.

(1) Armstrong, A. R.; Robertson, A. D.; Bruce, P. G. *J. Power Sources* **2005**, *146*, 275.
(2) Yu, D. Y. W.; Yanagida, K.; Kato, Y.; Nakamura, H. *J. Electrochem. Soc.* **2009**, *156*, A417.
(3) Johnson, C. S.; Kim, J.-S.; Lefief, C.; Li, N.; Vaughey, J. T.; Thackeray, M. M. *Electrochem. Commun.* **2004**, *6*, 1085.
(4) Thackeray, M. M.; Johnson, C. S.; Vaughey, J. T.; Li, N.; Hackney, S. A. *J. Mater. Chem.* **2005**, *15*, 2257.
(5) Johnson, C. S.; Li, N.; Lefief, C.; Thackeray, M. M. *Electrochem. Commun.* **2007**, *9*, 787.
(6) Park, S. H.; Kang, S.-H.; Johnson, C. S.; Amine, K.; Thackeray, M. M. *Electrochem. Commun.* **2007**, *9*, 262.
(7) Gao, J.; Kim, J.; Manthiram, A. *Electrochem. Commun.* **2009**, *11*, 84.
(8) Jarvis, C. R.; Lain, M. J.; Yakovleva, M. V.; Gao, Y. *J. Power Sources* **2006**, *162*, 800.

© 2010 American Chemical Society
Published on Web 01/11/2010

cell assembly in the discharged state. The second method was recently demonstrated by Novák et al.[9] and previously by David et al.[10] who prepared chemically lithiated (discharged) $Li_4V_3O_8$ and Li_2MnO_2 electrodes, respectively, which are air-sensitive and somewhat difficult materials to handle. The electrochemical data are compared with $C_6/Li_{1.2}V_3O_8-Li_2MnO_3$ lithium-ion cells containing a Li_2MnO_3 ($Li_2O\cdot MnO_2$) cathode precursor, which has a low Li_2O content relative to Li_5FeO_4 ($5Li_2O\cdot Fe_2O_3$). The implications of using Li_2O-containing metal oxide electrodes for lithium-air cells are briefly discussed.

II. Experimental Methods

An orange-colored Li_5FeO_4 product was prepared by (1) intimately mixing stoichiometric amounts of $LiOH\cdot H_2O$ (Aldrich, 99+%) with nanosized Fe_2O_3 (Aldrich, 99+%) and 2) firing the powders under flowing nitrogen at 800 °C for 72 h. Li_2MnO_3 was synthesized by the solid-state reaction of Li_2CO_3 (Aldrich, 99%) with $MnCO_3$ (Aldrich, 99%) powders in air at 500 °C for 40 h; $Li_{1.2}V_3O_8$ was prepared in a similar manner by reacting V_2O_5 (Aldrich, 99%) and $LiOH\cdot H_2O$ powders in air at 550 °C for 6 h. Because Li_5FeO_4 has a very high lithium content, it slowly decomposes in air, reacting with ambient moisture and CO_2. For this reason, care was taken to store and handle the Li_5FeO_4 samples in an inert atmosphere.

Chemical delithiation of Li_5FeO_4 was accomplished by reaction with nitronium tetrafluoroborate (NO_2BF_4, Aldrich, 98%) under nitrogen gas. Molar quantities of NO_2BF_4, which is an extremely strong oxidant with an oxidizing power of ~5.1 V vs lithium metal,[11] were used to extract 1, 2, 3 Li per Li_5FeO_4 unit; a slight excess of NO_2BF_4 was used to extract all the lithium (5 Li). The slow addition of solid NO_2BF_4 to Li_5FeO_4 in acetonitrile was accompanied immediately by gas evolution from the sample. The powders were stirred for 4−6 h at room temperature, vacuum filtered, and washed multiple times with acetonitrile. The Li/Fe ratio in the parent and delithiated samples was measured by inductively coupled plasma optical emission spectrometry (ICP-OES) at the Analytical Chemistry Laboratory (ACL) at Argonne.

Powder X-ray diffraction data of the various samples were collected with a Siemens D5000 diffractometer (Cu Kα radiation) at a scan rate of 0.6°2θ/min. For protection, the air-sensitive Li_5FeO_4 and chemically delithiated products were covered with an aluminized mylar film.

X-ray absorption spectroscopy (XAS) data of (1) the parent compound Li_5FeO_4, (2) chemically delithiated powders, (3) a charged Li_5FeO_4 electrode (in a sealed pouch cell) from which 2 Li had been extracted, and (4) an α-Fe_2O_3 (Fe^{3+}) standard were collected . For these experiments, samples were prepared by thoroughly mixing an appropriate amount of the powders with finely divided graphite and cold pressing the powders to make uniform pellets. The pellets were covered and sealed with two layers of aluminized mylar. All sample preparations were carried out in a helium glovebox. To avoid the ingress of air, XAS experiments were performed in a sample chamber with flowing helium gas. The Li/Li_5FeO_4 cell consisted of a lithium metal anode, a cathode laminate of Li_5FeO_4, and a porous polypropylene separator soaked with 1.2 M $LiPF_6$/ethylene carbonate: ethylmethyl carbonate (EC:EMC, 3:7 weight ratio) electrolyte, contained within a polypropylene-polyester pouch lined with an aluminum barrier. The current collectors for the Li anode and the Li_5FeO_4 cathode were a Ni mesh and an aluminum foil, respectively. The pouch cell was heat-sealed at the current leads. The XAS experiments were performed in Sector 20, bending magnet beamline (PNC/XOR, 20-BM) of the Advanced Photon Source at Argonne. Measurements at the Fe K-edge were performed in the transmission mode at room temperature using gas ionization chambers to monitor the incident and transmitted X-ray intensities. A third ionization chamber was used in conjunction with a bcc Fe-foil standard to provide internal calibration for the alignment of the edge position. Monochromatic X-rays were obtained using a fixed-exit Si (111) double crystal monochromator. The monochromator energy was calibrated using a Fe foil spectrum and setting the inflection point (first derivative maxima at the edge) to 7112.0 eV. A rhodium-coated X-ray mirror was used to suppress higher order harmonics. Care was taken to minimize distortions of the spectra from thickness effects. Data reduction was carried out using XAS analysis software developed by Ravel and Newville.[12]

To investigate the electrochemical behavior of the Li_5FeO_4 and Li_2MnO_3 cathode precursors, lithium-ion coin cells (Hohsen 2032) with a graphite (MAG-10) anode and a Li_5FeO_4 or Li_2MnO_3 cathode were constructed. Lithium-ion cells with physically blended $Li_5FeO_4-Li_{1.2}V_3O_8$ (1:1 molar ratio) and $Li_2MnO_3-Li_{1.2}V_3O_8$ (0.76:0.24 molar ratio) cathodes were also evaluated. As a control experiment to monitor the electrochemical behavior of the charged $Li_{1.2}V_3O_8$ component, $Li/Li_{1.2}V_3O_8$ half-cells were built using a Li metal-foil anode (FMC Lithium). In addition, a Li-half cell of Li_5FeO_4 was used to evaluate the lithium extraction process and to determine the maximum amount of lithium that could be removed electrochemically from the material at a slow (C/40) rate (0.05 mA/cm^2). The cathodes of all cells consisted typically of 80^w/o active mass (i.e. both Li_5FeO_4 or Li_2MnO_3 precursor, and, if present, the charged $Li_{1.2}V_3O_8$ component), 8^w/o PVDF binder, with 6^w/o graphite (SFG-6) and 6^w/o acetylene black as current collecting media. The electrolyte was a 1.2 M $LiPF_6$/EC:EMC (3:7) solution (Tomiyama). Because the Li_5FeO_4 and Li_2MnO_3 cathode precursors are electrochemically activated and react with lithium at different potentials, various upper and lower voltage limits were selected for the electrochemical tests. C_6/Li_5FeO_4 cells were charged and discharged between 3.8 and 1.0 V, whereas C_6/Li_2MnO_3 cells were cycled between 4.8 and 2.0 V. The $C_6/Li_5FeO_4-Li_{1.2}V_3O_8$ cells were initially charged to 4.5 V and discharged to 1.0 V, and then subsequently cycled between 4.5 and 1.0 V; $C_6/Li_2MnO_3-Li_{1.2}V_3O_8$ cells were charged and discharged between 4.7 and 1.0 V for two break-in cycles at 0.05 mA/cm^2 and subsequently cycled between 4.7 and 2.0 V at 0.1 mA/cm^2. $Li/Li_{1.2}V_3O_8$ half-cells were operated between 4.9 and 2.0 V. Cells were cycled at 0.1 mA/cm^2, unless otherwise specified.

III. Results and Discussion

Li_5FeO_4 and Delithiated Structure. Li_5FeO_4 has a defect antifluorite structure in which one Fe^{3+} ion substitutes for three Li^+ ions in Li_2O; it can be represented as $Li_5Fe\square_2O_4$, or $[Li_{1.25}Fe_{0.25}\square_{0.50}]O$, in which □ is a vacancy. Li_5FeO_4 has orthorhombic symmetry (*Pbca*) with

(9) Ng, S.-H.; Tran, N.; Bramnik, K. G.; Hibst, H.; Novák, P. *Chem.—Eur. J.* **2008**, *14*, 11141.
(10) David, W. I. F.; Goodenough, J. B.; Thackeray, M. M.; Thomas, M. G. S. R *Rev. Chim. Miner.* **1983**, *20*, 636.
(11) Elder, S. H.; Doerrer, L. H.; DiSalvo, F. J.; Parise, J. B.; Guyomard, D.; Tarascon, J. M. *Chem. Mater.* **1992**, *4*, 929.
(12) Ravel, B.; Newville, M. *J. Synch. Radiat.* **2005**, *12*, 537.

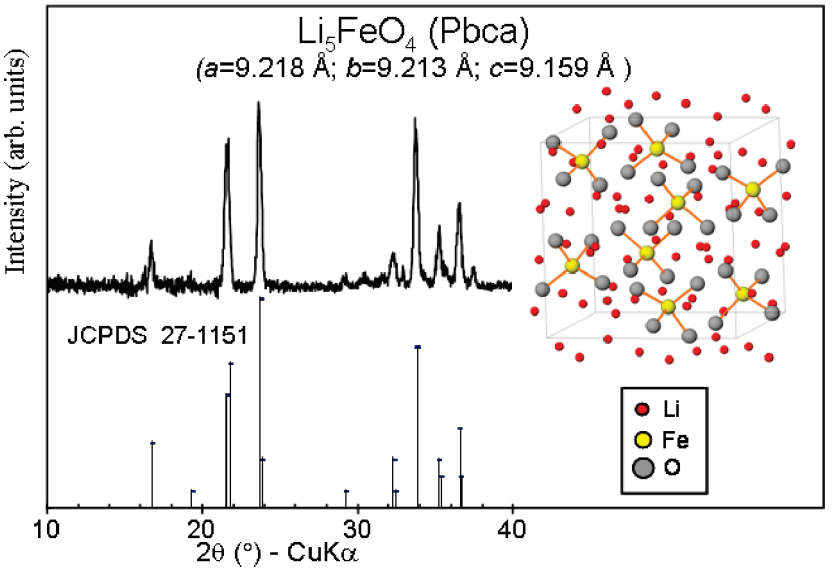

Figure 1. X-ray diffraction pattern and schematic structural representation of Li_5FeO_4.

lattice parameters of 9.218, 9.213, and 9.153 Å,[13] each of which is essentially double that of the "*a*" lattice parameter of cubic Li_2O ($Fm\bar{3}m$, a = 4.610 Å).[14] The X-ray diffraction pattern of the as-prepared Li_5FeO_4 sample obtained after standing in air for 8 h, as well as the JCPDS reference pattern[15] (to 37.5°2θ) and a schematic illustration of the structure are shown in Figure 1. The X-ray pattern shows a minor amount of Li_2CO_3 impurity (< 5%), as indicated by the weak peaks between 30 and 32°2θ (Cu Kα; 0.6°2θ/min). The Fe^{3+} ions in the Li_5FeO_4 structure reside in isolated FeO_4 tetrahedra, the lithium ions occupying 5/7 of the remaining tetrahedral sites. The interstitial tetrahedral and octahedral sites provide an energetically favorable pathway for fast Li^+-ion diffusion. The structure of layered Li_2MnO_3 and its electrochemical behavior have already been described in previous reports.[1−4]

The lithium content in the parent Li_5FeO_4 compound and chemically delithiated products, as determined by ICP-OES analysis, followed the expected trend for the starting material Li_5FeO_4 (Li/Fe = 5) and the removal of 0, 1, 2, 3, and 5 Li/per Li_5FeO_4 unit, yielding experimental values of x = 0, 0.94, 1.8, 2.64, and 4.94 in "$Li_{5-x}FeO_4$", respectively. (Note: the formula "$Li_{5-x}FeO_4$", which does not take into account the extent of oxygen loss from the sample, is used for simplicity throughout the paper for both chemically- and electrochemically delithiated samples.) The XRD patterns of the four samples ($0 \le x < 3$) that were protected from air by an aluminized mylar X-ray window, were obtained immediately after removal from the helium glovebox (Figure 2). For this compositional range, lithium extraction did not significantly alter the peak positions; however, noticeable changes in the relative peak intensities occurred (with the emergence of a

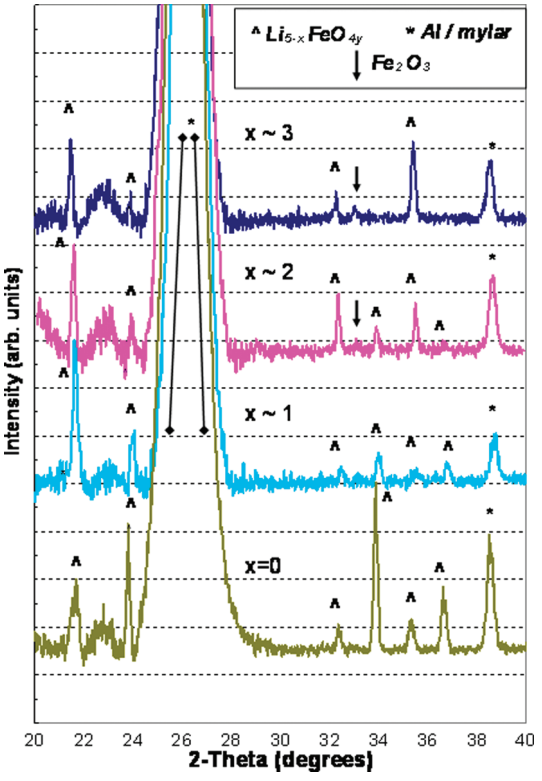

Figure 2. X-ray diffraction patterns of Li_5FeO_4 and chemically delithiated samples for the extraction of 0, ~1, ~2, and ~3 Li per Li_5FeO_4 unit.

weak peak at ~33°2θ, tentatively attributed to α-Fe_2O_3), providing evidence that lithium extraction was accompanied by iron diffusion within the cubic-close-packed oxygen array. Complete extraction of lithium (x = 4.94) yielded a featureless X-ray pattern, indicative of a fully delithiated iron oxide product that was amorphous to X-rays (not shown in Figure 2).

The XRD data of the chemically delithiated samples (x = ~1, 2, 3, and 5) were of insufficient quality to allow detailed structural analyses of the samples. Therefore, for

(13) Luge, R.; Hoppe, R *Z. Anorg. Allg. Chem.* **1984**, *513*, 141.
(14) Farley, T. W. D.; Hayes, W.; Hull, S.; Hutchings, M. T.; Vrtis, M. *J. Phys: Condens. Matter* **1991**, *3*, 4761.
(15) JCPDS data file, No. 27-1151.

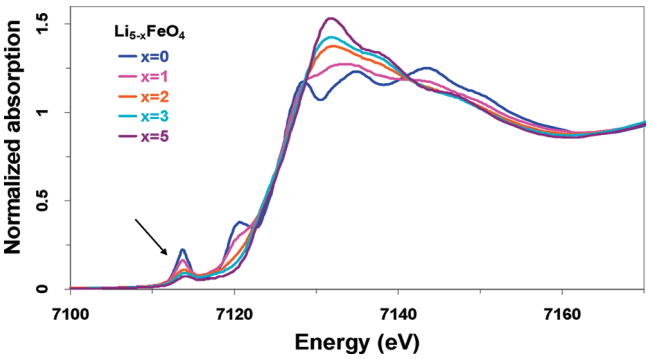

Figure 3. Fe *K*-edge XANES of chemically delithiated Li_5FeO_4 samples for the extraction of approximately 0, 1, 2, 3, and 5 Li per Li_5FeO_4 unit. The pre-edge feature is indicated by an arrow.

this study, X-ray absorption near edge spectra (XANES) data of the samples were collected because they can provide valuable information about the electronic structure and are sensitive to the oxidation state and coordination symmetry of the iron ions (Figure 3). The XANES spectrum of Li_5FeO_4 shows a strong pre-edge peak feature (indicated by an arrow in Figure 3), which is characteristic of tetrahedrally coordinated Fe^{3+} ions in metal oxides.[16] The strong intensity of the pre-edge peak arises because tetrahedral sites do not possess an inversion center of symmetry. The assignment of tetrahedrally coordinated Fe^{3+} in Li_5FeO_4 is consistent with the crystal structure of this compound. As lithium is removed by chemical delithiation, the shape of the spectra changes systematically as a function of lithium content ($x = \sim 1$ to $x = \sim 5$). In particular, the intensity of the pre-edge gradually decreases with increasing x, that is, as more lithium is extracted from the structure. If lithium extraction occurs with faradaic charge transfer on the iron ions, that is, as $Li_{5-x}FeO_4$, then one would expect all the iron ions to be tetravalent, Fe^{4+}, in Li_4FeO_4 ($x = 1$). In a XANES spectrum, the presence of Fe^{4+} ions in tetrahedral sites would likely lead to an increased intensity of the pre-edge peak (due to a larger d-hole count) as well as a shift to higher energy values when compared to Li_5FeO_4, whereas the presence of Fe^{4+} in octahedral coordination would lead to a significant reduction in pre-edge peak intensity. In metal oxides with octahedrally coordinated iron, the pre-edge is composed of many peaks (arising from empty t_{2g} and e_g states as well as other nonlocal interactions); however, due to the more centro-symmetric environment in these compounds the pre-edge intensity is not large. We therefore infer from the XANES data in Figure 3 that, in the chemically prepared Li_4FeO_4 sample, a charge compensation mechanism other than the oxidation of Fe^{3+} to Fe^{4+} takes place, with the caveat that any Fe^{4+} that is formed during the initial stage of the reaction, at least for the extraction of one Li, is perhaps transient in nature and is not present in the fully equilibrated sample. This premise is supported by the highly oxidizing power of NO_2BF_4 (equivalent to ~5.1 V vs metallic lithium[11]), which is likely to strip both lithium and oxygen simultaneously from the surface of the Li_5FeO_4 structure. Furthermore, a comparison of the position and intensity of the pre-edge peak of the fully delithiated compound ($x = \sim 5$) with standard iron oxide materials strongly suggest that the iron ions are present predominantly as octahedrally coordinated Fe^{3+} ions.[16,17] In other words, the spectra of the chemically delithiated samples do not exhibit XANES features that would be consistent with the presence of significant amounts of octahedrally coordinated Fe^{4+} ions; in this respect, the presence of Fe^{4+} would likely result in a significantly higher pre-edge/edge position, as observed in other formally tetravalent Fe^{4+} compounds,[18] such as fully oxygenated $SrFeO_3$. Therefore, our conclusion from these studies is that chemical delithiation of Li_5FeO_4 is accompanied by oxygen loss to maintain the trivalent oxidation state of iron, leaving $Li_{5-2y}FeO_{4-y}$ products ($0 < y < 2.5$). The net result is a loss of Li_2O from the Li_5FeO_4 ($5Li_2O \cdot Fe_2O_3$) structure that occurs with (1) a concomitant increase of Fe_2O_3 in the delithiated product, (2) the migration of the Fe^{3+} ions from tetrahedral- to octahedral sites, and (3) the condensation of the isolated FeO_4 tetrahedra to a polyhedral linkage with Fe−Fe correlations at the expected distance for edge−shared FeO_6 octahedra. On complete delithiation ($y = 2.5$), the reaction would be simply:

$$2Li_5FeO_4 \rightarrow Fe_2O_3 + 5Li_2O \qquad (1)$$

X-ray absorption experiments were also carried out on an electrochemically delithiated sample under open-circuit-voltage (OCV) conditions. This sample was prepared by charging a Li/Li_5FeO_4 pouch cell to remove ~2 Li from the Li_5FeO_4 electrode (i.e., a capacity of ~340 mAh/g), and allowing the cell to relax for ~24 h before the XAS data were recorded. The OCV of the cell was 3.17 V during the data collection. The normalized Fe K-edge XANES spectra of the delithiated samples (Figure 4(a)) show significant changes in position and shape relative to the original Li_5FeO_4. As described earlier, a systematic reduction in pre-edge peak intensity shows a gradual conversion of Fe^{3+} from tetrahedral to octahedral symmetry in the chemically delithiated samples (Figure 3). In the electrochemically delithiated sample, the position of the main edge is shifted to higher energies when compared to the chemically delithiated sample. Comparison of the pre-edge peak shows that the spectral weight is shifted to higher energy values and the pre-edge peak has higher intensity in the electrochemically prepared sample relative to the chemically delithiated sample. These observations provide evidence of oxidized iron formation on electrochemically removing lithium from the Li_5FeO_4 structure. Similar trends are seen in the XANES of other systems which exhibit oxidation of trivalent Fe^{3+} to

(16) Wilke, M.; Farges, F.; Petit, P.-E.; Brown, G. E.Jr.; Martin, F. *Am. Mineral.* **2001**, *86*, 714.

(17) Jain, G.; Balasubramanian, M.; Xu, J. J. *Chem. Mater.* **2006**, *18*, 423.

(18) Vracar, M.; Kuzmin, A.; Merkle, R.; Purans, J.; Kotomin, E. A.; Maier, J.; Mathon, O. *Phys. Rev. B* **2007**, *76*, 174107.

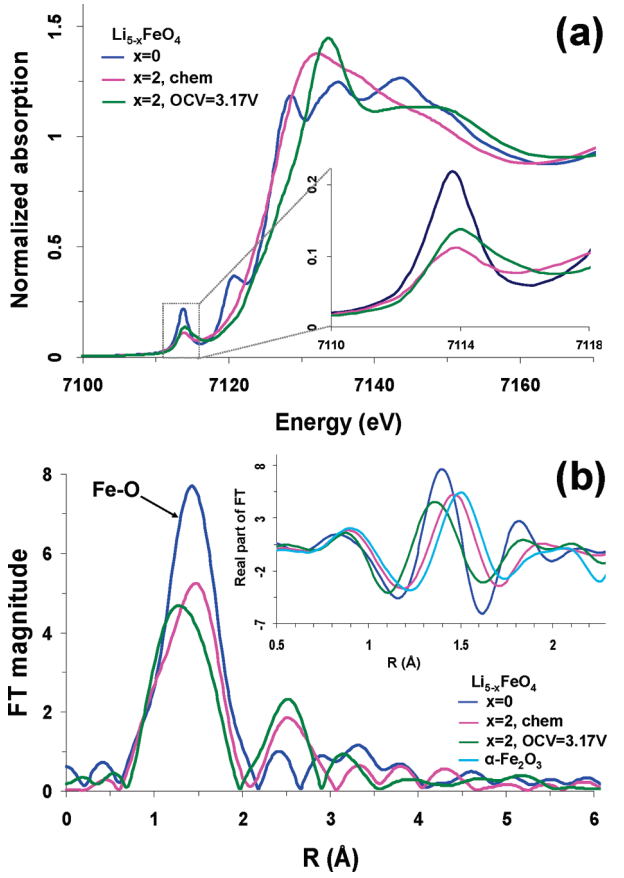

Figure 4. (a) Fe *K*-edge XANES (inset: pre-edge) and (b) k^3-weighted Fourier Transform magnitude (inset: real part of FT) of EXAFS spectra for Fe in as prepared Li_5FeO_4 ($x = 0$), chemically delithiated $Li_{5-x}FeO_4$ ($x = 2$), electrochemically charged ($x = 2$) Li/Li5FeO4 pouch cell, OCV = 3.17 V. Data for $\alpha-Fe_2O_3$ has also been shown in the real part of FT as a standard for comparison. The k range of FT is 3.5−10 $Å^{-1}$.

tetravalent Fe^{4+}.[18−21] Further evidence is obtained by a qualitative comparison of the EXAFS data. The k^3-weighted Fourier transform (FT) magnitude of EXAFS spectra is shown in Figure 4(b). The first peak in the 1−2 Å range arises from contributions involving the first Fe−O correlation. An expanded view of the real part of the FT (which contains both phase and amplitude information) in the region of the Fe−O correlation is shown in the inset. Data from $\alpha-Fe_2O_3$ and pristine Li_5FeO_4 are added as standards for Fe^{3+} in octahedral and tetrahedral symmetry respectively. The average Fe−O bond distance for Fe^{3+} in octahedral coordination with O is ∼2.00 Å, whereas the Fe−O bond distance for Fe^{3+} in tetrahedral coordination is ∼1.89 Å.[17,18] This difference in bond distance is evident in the real part of the FT, where the contribution from the Fe−O correlation occurs at significantly higher *r*-values for $\alpha-Fe_2O_3$ relative to Li_5FeO_4. In the chemically delithiated sample, the contribution of the Fe−O correlation is intermediate to that of the two standards, consistent with the partial conversion of tetrahedral Fe^{3+} to octahedral Fe^{3+}. In sharp contrast for the electrochemically prepared sample, the contribution of the Fe−O correlation occurs at lower *r*-values. Oxidation of Fe^{3+} to Fe^{4+} in octahedral coordination with oxygen, leads to a reduction in the average Fe−O bond distance by ∼0.12−0.15 Å.[18−21] Similarly, in tetrahedral symmetry, the average Fe−O bond distance decreases by ∼0.09 Å on oxidation from Fe^{3+} to Fe^{4+}.[22] Inspection of the real part of the FT clearly shows that on removal of similar moles of Li ($x = 2$), the average Fe−O bond distance in the electrochemically prepared sample is much smaller. In conjunction with the XANES data, the presence of a lower average Fe−O bond distance reveals the presence of oxidized iron in the electrochemically prepared sample. Fe^{4+} formation is expected to occur predominantly during the electrochemical removal of the first Li^+ ion. Note, however, that our XAS data were collected after removal of ∼2 Li^+ ions, so other charge compensation mechanisms must be taken into consideration, such as (1) oxygen loss from the sample (effective Li_2O removal), which would be consistent with the results of our chemically delithiated samples, or (2) perhaps the further oxidation of iron to a metastable (transient) state beyond $x = 1$ in $Li_{5-x}FeO_4$. Also, due to the $3d^4$ electronic configuration, Fe^{4+} ions can exhibit a Jahn−Teller distortion. To monitor the Fe^{4+} oxidation process and to understand the additional charge-compensation mechanisms during electrochemical charging requires a systematic study of the evolution of electronic and atomic structures. In-situ XAS studies of $Li_{5-x}FeO_4$ electrodes during charging are currently underway at Argonne's Advanced Photon Source, the results of which will be reported subsequently with more detailed analyses of the EXAFS data.

Li/Li_5FeO_4, C_6/Li_5FeO_4, C_6/Li_2MnO_3, and Li/LiV_3O_8 Cells. The electrochemical properties of Li_5FeO_4 were first investigated by Nurakawa et al.[23] and subsequently by Obrovac et al.[24] and Imanishi et al.[25] in lithium cells using a Li metal counter electrode. Obrovac et al.[24] demonstrated that when Li/Li_5FeO_4 cells are initially discharged, lithium is inserted into the Li_5FeO_4 structure below 1 V with simultaneous iron extrusion, yielding ∼700 mAh/g; thereafter, the electrode delivers a reversible capacity of approximately 200 mAh/g when cycled between 3.0 and 0 V. Nurakawa et al.[23] and Imanishi et al.[25] (the latter using Mossbauer spectroscopy) concluded from their experiments, in which lithium was first extracted from the Li_5FeO_4 electrode, that a reversible capacity of approximately one Li per Fe (173 mAh/g; charge/discharge limited to one Li) could be achieved and that the redox behavior could be attributed to a $Fe^{3+/4+}$ couple; higher levels of lithium extraction were proposed

(19) Holzapfel, M.; Proux, O.; Strobel, P.; Darie, C.; Borowskie, M.; Morcrette, M. *J. Mater. Chem.* **2004**, *14*, 102.
(20) Mansour, A. N.; Croguennec, L.; Pradob, G.; Delmas, C. J. Synchrotron Radiat. **2001**, *8*, 866.
(21) Blasco, J.; Aznar, B.; García, J.; Subías, G.; Herrero-Martín, J.; Stankiewicz, J. *Phys. Rev. B* **2008**, *77*, 054107.
(22) Weller, M. T.; Hecto, A. L. *Angew. Chem., Int. Ed.* **2000**, *39*(22), 4162.
(23) Narukawa, S.; Takeda, Y.; Nishijima, M.; Imanishi, N.; Yamamoto, O.; Tabuchi, M. *Solid State Ionics* **1999**, *122*, 59.
(24) Obrovac, M. N.; Dunlap, R. A.; Sanderson, R. J.; Dahn., J. R. *J. Electrochem. Soc.* **2001**, *148*, A576.
(25) Imanishi, N.; Inoue, A.; Hirano, A.; Ueda, M.; Takeda, Y.; Sakaeba, H.; Tabuchi, M. *J. Power Sources* **2005**, *146*, 21.

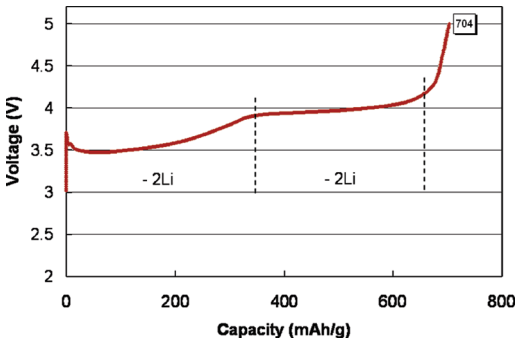

Figure 5. Voltage profile of a Li/Li_5FeO_4 cell for the initial electrochemical extraction of Li at a slow C/40 (0.05 mA/cm^2) rate.

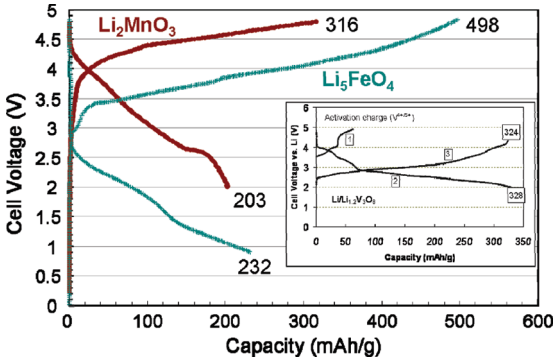

Figure 6. Initial charge and discharge profiles of C_6/Li_5FeO_4, C_6/Li_2MnO_3, and $Li/Li_{1.2}V_3O_8$ (inset) cells.

to lead to structural decomposition. Therefore, our EXAFS data, that provide evidence of some Fe^{4+} in electrochemically delithiated samples are consistent with the Mossbauer data of $Li_{5-x}FeO_4$ electrodes, for $x < 1$, reported by Imanishi et al.[25]

Charging our Li/Li_5FeO_4 cells to 5 V at a slow C/40 rate (0.05 mA/cm^2) shows that lithium removal takes place in two steps, the first between ~3.5 and 4.0 V and the second on a voltage plateau at 4 V, each step corresponding to the removal of one Li_2O per Li_5FeO_4 formula unit (Figure 5). Therefore, the capacity delivered by these two processes in total (~690 mAh/g) corresponds to 80% of the theoretical capacity (867 mAh/g), or 4 Li per Li_5FeO_4 formula unit. Assuming that tetravalent iron is a transient, metastable oxidation state and that on equilibration at a slow current rate, lithium is extracted with oxygen from Li_5FeO_4 as Li_2O, the net composition $Li_{5-2y}FeO_{4-y}$ at $y = 2$ (4 Li) would be $LiFeO_2$, which is a stable rocksalt composition. The sharp increase in voltage after the removal of 4 Li from the Li_5FeO_4 structure, strongly suggests that $LiFeO_2$ is the limiting composition beyond which further extraction of Li_2O becomes very difficult. Nevertheless, the large accessible capacity (~700 mAh/g) renders Li_5FeO_4 an attractive precursor material for supplying the negative electrode (anode) of lithium-ion cells (e.g., graphite) with lithium during the initial charge before the onset of significant electrolyte oxidation (> 4.2 V), and for using the surplus capacity loaded into the anode to discharge a charged component (e.g., $Li_{1.2}V_3O_8$) combined with the Li_5FeO_4 precursor in the parent cathode. Clearly, in such an example, the amounts of the Li_5FeO_4 precursor, the charged $Li_{1.2}V_3O_8$ cathode component and the graphite anode need to be carefully balanced to ensure optimum functioning of the lithium-ion cell.

The electrochemical profile of the initial charge/discharge cycle of a C_6/Li_5FeO_4 lithium-ion cell with a Li_5FeO_4 cathode precursor for loading the graphite anode with lithium at a 0.1 mA/cm^2 rate (which is twice that used in Figure 5) is compared with that of a C_6/Li_2MnO_3 cell in Figure 6. Although the initial charge/discharge behavior of the Li_5FeO_4 electrode is consistent with the results of Nurakawa et al.[23] and Imanishi et al.,[25] our data show that when charged to 4.8 V, 498 mAh/g could be withdrawn from Li_5FeO_4. In the absence of electrolyte effects, the capacity of the Li_5FeO_4 electrode in this example corresponds to the removal of approximately 3 Li per Fe (519 mAh/g) (or 1.5 Li_2O per Li_5FeO_4 unit), that is, 60% of the theoretical capacity (867 mAh/g). Discharge of the C_6/Li_5FeO_4 cell takes place in two steps, the first between 2.6 and 1.5 V (~100 mAh/g) and the second between 1.5 and 1.0 V (~132 mA/g). The first step of the discharge process (2.6−1.5 V) is tentatively attributed to lithium insertion into the residual $Li_{5-2y}FeO_{4-y}$ ($y < 1.5$) structure with a concomitant reduction of trivalent to divalent iron; the second step of the reaction (below 1.5 V) is attributed to the extrusion of iron and its reduction to the metallic state.[26]

Lithium extraction from Li_5FeO_4 (as Li_2O) occurs at a significantly lower voltage than it does for Li_2MnO_3 (Figure 6), which suggests that the structure type influences oxygen removal. In this respect, Li_5FeO_4 has an ionic structure with lithium ions surrounded by isolated $[FeO_4]^{3-}$ tetrahedra, whereas Li_2MnO_3 contains lithium ions within a more strongly bonded, edged-shared network of MnO_6 octahedra. In the latter case, only 316 mAh/g, which corresponds to the removal of ~1.38 Li per Mn, (i.e., 69% of the theoretical value for complete Li_2O removal, 459 mAh/g) was withdrawn from the electrode between 3 V and the upper cutoff limit (4.8 V). On discharge to 2 V, the delithiated Li_2MnO_3 electrode delivered 204 mAh/g, corresponding to the reinsertion of 0.9 Li per Mn unit; the short plateau toward the end of discharge at 2.6 V suggests the conversion of the layered structure to spinel, which has been observed in previous electrochemical studies of delithiated Li_2MnO_3.[3] The capacity delivered by the Li_2MnO_3 precursor between 3 and 4.4 V on the initial charge and the reintroduction of 0.9 Li per Mn during discharge indicates a final Mn oxidation state of 3.1 in the discharged product.

The charge/discharge profile of a $Li/Li_{1.2}V_3O_8$ lithium half cell is provided as an inset in Figure 6. It shows the typical electrochemical behavior of, and capacity delivered by, the charged $Li_{1.2}V_3O_8$ cathode component used in this study.[27] The $Li/Li_{1.2}V_3O_8$ cell was charged first to 4.8 V to fully oxidize the vanadium ions to the pentavalent

(26) Thackeray, M. M.; Bruce, P. G.; Goodenough, J. B. *Mater. Res. Bull.* **1982**, *17*, 785.
(27) Pistoia, G.; Pasquali, M.; Tocci, M.; Moshtev, R. V.; Manev, V. *J. Electrochem. Soc.* **1985**, *132*, 281.

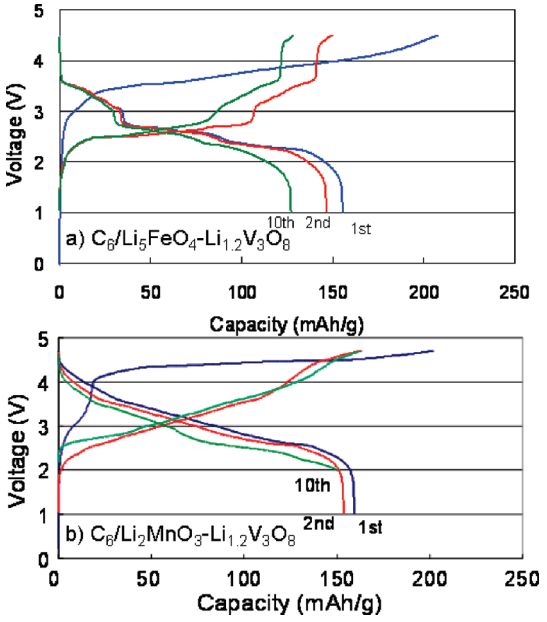

Figure 7. Cycling performance of (a) $C_6/Li_5FeO_4-Li_{1.2}V_3O_8$ and (b) $C_6/Li_2MnO_3-Li_{1.2}V_3O_8$ lithium-ion cells.

state (process 1 in Figure 6). (Note: the initial two-step process and delivered electrochemical capacity (40 mAh/g) indicate the likelihood that the parent $Li_{1.2}V_3O_8$ electrode was slightly oxygen deficient, thereby accounting for the slightly larger-than-expected capacity withdrawn between 3.5 and 4.5 V; the extraction of 0.2 Li from $Li_{1.2}V_3O_8$ would deliver only 19 mAh/g). The subsequent discharge/charge profile of the cell (processes 2 and 3) demonstrates that more than 300 mAh/g can be delivered reversibly by the $Li_{1.2}V_3O_8$ electrode between 4.8 and 2.0 V. Therefore, our electrochemical results in Figure 5 indicate that if more than 300 mAh/g can be withdrawn from the Li_5FeO_4 and Li_2MnO_3 precursor electrodes to charge the graphite anode of a lithium-ion cell, and if this capacity can be recovered by the activated precursor and a charged cathode component such as $Li_{1.2}V_3O_8$ during discharge, then it should be possible to engineer lithium-ion cells with blended and balanced Li_5FeO_4 (or Li_2MnO_3) and $Li_{1.2}V_3O_8$ cathode components that together can deliver at least 150 mAh/g when cycled between 4.8 and 1.5 V, particularly if the mass of Li_2O lost during the activation of the precursor electrodes is taken into consideration.

$C_6/Li_5FeO_4-Li_{1.2}V_3O_8$ and $C_6/Li_2MnO_3-Li_{1.2}V_3O_8$ Lithium-Ion Cells. The electrochemical cycling profiles for the 1st to 10th cycles of $C_6/Li_5FeO_4-Li_{1.2}V_3O_8$ and $C_6/Li_2MnO_3-Li_{1.2}V_3O_8$ lithium-ion cells, are shown in Figures 7a and b, respectively. A Li_5FeO_4:$Li_{1.2}V_3O_8$ molar ratio of 1:1 was selected for the $C_6/Li_5FeO_4-Li_{1.2}V_3O_8$ cell, whereas a Li_2MnO_3:$Li_{1.2}V_3O_8$ molar ratio of 0.74:0.26 was selected for the $C_6/Li_2MnO_3-Li_{1.2}V_3O_8$ cell to compensate for the lower Li_2O content in the Li_2MnO_3 precursor relative to Li_5FeO_4.

The electrochemical profiles of the initial charge/discharge cycles of the lithium-ion cells in Figures 7a and b are a combination of the C_6/Li_5FeO_4, C_6/Li_2MnO_3, and $Li/Li_{1.2}V_3O_8$ voltage profiles shown in Figure 6. In Figure 7a, taking into consideration (1) the individual capacities from the blended $Li_5FeO_4-Li_{1.2}V_3O_8$ components when charged to 4.5 V, (2) the relative masses of the components, and (3) probable electrolyte oxidation effects at potentials approaching 4.5 V, the initial charge capacity of 208 mAh/g is in good agreement with the expected capacity of 205 mAh/g delivered by the independent C_6/Li_5FeO_4 and $Li/Li_{1.2}V_3O_8$ cells. The results demonstrate, in particular, the effectiveness of using a Li_5FeO_4 cathode precursor to load the graphite anode with lithium. When subsequently discharged to 2 V, lithium insertion into the activated Li_5FeO_4 and $Li_{1.2}V_3O_8$ components provides a capacity 156 mAh/g, reflecting a first-cycle efficiency of 75%. Thereafter, when cycled between 3.8 and 1.5 V, cells lost capacity steadily yielding 140−127 mAh/g over the next 10 cycles. The steady loss in capacity is attributed to irreversible iron extrusion from the iron-oxide component toward the end of discharge, and nonoptimized LiV_3O_8 highlighting the importance of tailoring the upper and lower voltage limits to optimize electrochemical performance, and electrode fabrication.

The electrochemical cycling behavior of the $C_6/Li_2MnO_3-Li_{1.2}V_3O_8$ lithium-ion cell is shown in Figure 7b, for comparison. In this case, using the electrochemical data in Figure 6 as a guide, notably (1) the level of lithium extraction from the Li_2MnO_3 precursor, that is, 1.38 Li per Li_2MnO_3 unit and (2) the corresponding capacity from the $Li_{1.2}V_3O_8$ electrode, then a maximum 187 mAh/g would be expected from the composite cathode when charged to 4.7 V, in good agreement with the experimentally obtained value (200 mAh/g, Figure 7b). When discharged to 1 V at 0.05 mA/cm^2 on the subsequent two cycles, the activated $Li_2MnO_3-Li_{1.2}V_3O_8$ cathode delivered > 150 mAh/g. Because this cathode delivered no significant capacity between 2 and 1 V, the lower voltage limit was raised to 2 V for further cycling, which was conducted at double the rate (0.1 mA/cm^2). Despite the narrower voltage range and slight decrease in discharge voltage due to polarization, the $Li_2MnO_3-Li_{1.2}V_3O_8$ cathode provided a steady 150 mAh/g for the next eight cycles, demonstrating superior cycling stability compared to $Li_5FeO_4-Li_{1.2}V_3O_8$. What is perhaps remarkable is that our results demonstrate that the Li_2MnO_3 component shows enhanced cycling stability when blended with $Li_{1.2}V_3O_8$, relative to its poor cycling efficiency as an independent electrode.[3]

Finally, the results presented in this study raise the interesting possibility of exploiting reversible Li_2O extraction/Li_2O reformation reactions in lithium-air cells. For example, our data demonstrate that Li_2O extraction from Li_5FeO_4 occurs predominantly between 3.5 and 4.0 V vs metallic lithium, which is considerably lower than the Li_2O_2 decomposition potentials reported by Bruce et al. in his studies of Li/O_2 cells with various metal oxide catalysts.[28,29] Our initial studies have recently demonstrated

(28) Debart, A.; Bao, J.; Armstrong, G.; Bruce, P. G. *J. Power Sources* **2007**, *174*, 1177.
(29) Debart, A.; Paterson, A. J.; Bao, J.; Bruce, P. G. *Angew. Chem., Int. Ed.* **2008**, *47*, 4521.

the possibility of designing a reversible $Li/Li_5FeO_4-O_2$ cell in which Li_2O is first electrochemically extracted from the Li_5FeO_4 component and reformed in the residual, delithiated cathode by introducing oxygen into the cathode compartment on the subsequent discharge. These studies are still in progress, the results of which will be reported in due course.

Conclusions

Li_5FeO_4 and Li_2MnO_3 have been evaluated as cathode precursors to load the graphite anode of $C_6/Li_5FeO_4-Li_{1.2}V_3O_8$ and $C_6/Li_2MnO_3-Li_{1.2}V_3O_8$ lithium-ion cells, in which a charged $Li_{1.2}V_3O_8$ component in the parent cathode is used to accommodate the surplus lithium provided to the anode during the initial charge of the cells. These composite lithium metal oxide electrodes containing manganese, vanadium and iron provide a capacity of at least 150 mAh/g, when cycled between 4.7 and 2 V; they offer the possibility of designing alternative lithium-ion battery cathodes without costly cobalt- and nickel components that are unstable in their charged states. Improvements to the capacity and cycling stability of the electrodes can be expected by tailoring their composition and the conditions under which the cells operate, for example, electrode and cell balancing and the optimization of upper and lower voltage limits. This work also has implications for using other defect antifluorite materials, such as Li_6MnO_4, as a source of lithium for loading lithium-ion cells in combination with other charged cathode materials, such as MnO_2. The results also raise interesting possibilities for exploiting reversible Li_2O extraction/Li_2O reformation reactions in lithium-air cells.

Acknowledgment. Financial support from the Office of Vehicle Technologies of the U.S. Department of Energy (DOE) is gratefully acknowledged. PNC/XOR facilities at the Advanced Photon Source, and research at these facilities, are supported by the U.S. Department of Energy - Basic Energy Sciences, a Major Resources Support grant from NSERC, the University of Washington, Simon Fraser University and the Advanced Photon Source. The submitted manuscript has been created by UChicago Argonne, LLC, Operator of Argonne National Laboratory ("Argonne"). Argonne, a U.S. Department of Energy Office of Science laboratory, is operated under Contract No. DE-AC02-06CH11357. The U.S. Government retains for itself, and others acting on its behalf, a paid-up, nonexclusive, irrevocable worldwide license in said article to reproduce, prepare derivative works, distribute copies to the public, and perform publicly and display publicly, by or on behalf of the Government.